

## Effects of adsorbed molecular ordering to the superconductivity of a two-dimensional atomic layer crystal

Shunsuke Inagaki,<sup>1</sup> Narunori Ebara,<sup>1</sup> Takahiro Kobayashi,<sup>2</sup> Ryota Itaya<sup>ⓧ</sup>,<sup>1</sup> Kenta Yokota<sup>ⓧ</sup>,<sup>3,4</sup>  
 Isamu Yamamoto<sup>ⓧ</sup>,<sup>5</sup> Jacek Osiecki<sup>ⓧ</sup>,<sup>6</sup> Khadiza Ali<sup>ⓧ</sup>,<sup>7</sup> Craig Polley,<sup>6</sup>  
 H. M. Zhang<sup>ⓧ</sup>,<sup>8</sup> L. S. O. Johansson,<sup>8</sup> Takashi Uchihashi<sup>ⓧ</sup>,<sup>3,4</sup> and Kazuyuki Sakamoto<sup>ⓧ</sup>,<sup>1,9,10,\*</sup>

<sup>1</sup>Department of Applied Physics, Osaka University, Osaka 565-0871, Japan

<sup>2</sup>Department of Material and Life Science, Osaka University, Osaka 565-0871, Japan

<sup>3</sup>Graduate School of Science, Hokkaido University, Sapporo 060-0810, Japan

<sup>4</sup>International Center for Materials Nanoarchitectonics (WPI-MANA), National Institute for Materials Science, Ibaraki 305-0044, Japan

<sup>5</sup>Synchrotron Light Application Center, Saga University, Saga 840-8502, Japan

<sup>6</sup>MAX IV Laboratory, Lund University, 221 00 Lund, Sweden

<sup>7</sup>Department of Microtechnology and Nanoscience, Chalmers University of Technology, 412 96 Göteborg, Sweden

<sup>8</sup>Department of Engineering and Physics, Karlstad University, 651 88 Karlstad, Sweden

<sup>9</sup>Spintronics Research Network Division, Institute for Open and Transdisciplinary Research Initiatives,  
 Osaka University, Osaka 565-0871, Japan

<sup>10</sup>Center for Spintronics Research Network, Osaka University, Osaka 560-8531, Japan



(Received 16 December 2022; accepted 2 February 2023; published 21 February 2023)

The effect of 3,4,9,10-perylenetetracarboxylic dianhydride (PTCDA) adsorption on the physical properties of the two-dimensional (2D) atomic layer superconductor (ALSC) In/Si(111)-( $\sqrt{7} \times \sqrt{3}$ ) has been studied by angle-resolved photoelectron spectroscopy, transport measurements, and scanning tunneling microscopy. Hole doping from the adsorbed molecules has been reported to increase the superconducting transition temperature  $T_c$  of this ALSC, and the molecular spin tends to decrease it. Owing to its large electron affinity and its nonexistent spin state, the adsorption of PTCDA was expected to increase  $T_c$ . However, the PTCDA adsorption dopes only a small number of holes in the In layers and causes a suppression of  $T_c$  with a sharp increase in the normal-state sheet resistance followed by an insulating transition. Taking the disordering of the arrangement of PTCDA into account, we conclude that the increase in resistance is due to the localization effect originating from the random potential that is induced by the disordered PTCDA molecules. The present result also indicates the importance of the crystallinity of a 2D molecular film adsorbed on ALSCs.

DOI: [10.1103/PhysRevMaterials.7.024805](https://doi.org/10.1103/PhysRevMaterials.7.024805)

### I. INTRODUCTION

In the past few decades, atomic layer superconductors (ALSCs) epitaxially grown on semiconductor surfaces have been intensively studied as a very fascinating platform for understanding the physical properties of two-dimensional (2D) superconductors (SCs) [1–6]. Intriguing physical phenomena, which require understanding beyond a three-dimensional conventional SC [7], have been reported for such 2D systems, e.g., enhanced in-plane critical magnetic field above the Pauli paramagnetic limit [8–11]. Furthermore, the combination of spin physics, which arises from the presence of both the spin-orbit coupling and broken inversion symmetry, with superconductivity has the possibility of the creation of novel superconducting states [12,13]. In terms of applications as well as fundamental science, further development of this field demands improvement and control of superconducting properties.

By utilizing the high sensitivity of ALSCs to surface adsorbates, a new method for tuning the superconducting transition temperature  $T_c$  by constructing 2D heterostructures consisting of an ALSC and well-ordered organic molecules was reported [14]. In this previous study, two different metal phthalocyanines, CuPc and MnPc, were adsorbed on the ALSC In/Si(111)-( $\sqrt{7} \times \sqrt{3}$ ) [referred to as ( $\sqrt{7} \times \sqrt{3}$ )-In hereafter]. ( $\sqrt{7} \times \sqrt{3}$ )-In consists of a double In atomic layer on Si(111) and forms a ( $\sqrt{7} \times \sqrt{3}$ ) supercell with a quasisquare lattice [15–17]. It has spin-polarized metallic surface bands in the normal state [18,19] and becomes superconducting at approximately 3 K [1–3,20,21]. Even though the two phthalocyanine molecules form similar ordered structures on ( $\sqrt{7} \times \sqrt{3}$ )-In,  $T_c$  was found to be enhanced by 5% with the use of CuPc, while  $T_c$  was rapidly suppressed in the case of MnPc adsorption. This  $T_c$  modification was explained as the consequence of a competition between a positive effect of hole doping [22] from the molecules into ( $\sqrt{7} \times \sqrt{3}$ )-In and a negative effect of the exchange interaction between the conduction-electron spin and the local spin in the molecules. However, no organic molecules except CuPc and ZnPc have ever been reported to increase  $T_c$  [14,23–25]. In order to

\*kazuyuki\_sakamoto@ap.eng.osaka-u.ac.jp

fully understand the effect of molecular adsorption on the physical properties of ALSCs, further investigations using different types of organic molecules are needed. 3,4,9,10-perylenetetracarboxylic dianhydride (PTCDA) is known to form highly ordered layers on several metal surfaces [26,27] and thus has been used as a prototypical molecule to study properties at the organic molecule-metal interface. Furthermore, PTCDA is also used as an electron acceptor due to its large electron affinity, whose value is much larger than that of CuPc in the isolated state [28,29] and has no spin states. This means that PTCDA would be a potential candidate to achieve a higher  $T_c$  of  $(\sqrt{7} \times \sqrt{3})$ -In.

In this paper, we report the electronic structure, conductivity, and atomic structure of PTCDA adsorbed  $(\sqrt{7} \times \sqrt{3})$ -In, which were established by high-resolution angle-resolved photoelectron spectroscopy (ARPES), transport measurements, and scanning tunneling microscopy (STM), respectively. Although a large amount of hole doping and an increase in  $T_c$  were expected from the electronic properties of PTCDA, only a small amount of hole doping and a suppression of  $T_c$  were observed. Moreover, a sharp increase in the normal-state resistance that eventually undergoes an insulating transition without destruction of the metallic character of  $(\sqrt{7} \times \sqrt{3})$ -In was observed. Taking the disordering of adsorbed PTCDA into account, we conclude that the suppression of superconductivity and the insulating transition are due to the random potentials induced by the disordered arrangement of PTCDA molecules, which would scatter the conduction electrons and cause carrier localization in the 2D In layer. Our findings suggest that molecular films with high crystalline quality are indispensable for improving the superconductivity in 2D systems consisting of an ALSC and organic molecules.

## II. EXPERIMENTAL DETAILS

High-resolution ARPES measurements were conducted at the Bloch beamline of MAX IV, Sweden, which is equipped with a DA30-L analyzer (Scienta Omicron), and beamline 13 of Saga Light Source, Japan, equipped with an A-1 analyzer (MB Scientific AB). The transport experiment was performed using the four-point probe method in a home-built ultrahigh vacuum (UHV) apparatus [2,20], and the STM observation was done using a low-temperature STM (UNISOKU Co. Ltd.). An *n*-type Si(111) substrate (1–5  $\Omega$  cm) was used for photoelectron spectroscopy (PES) and low-temperature STM, and a nondoped one (>1000  $\Omega$  cm) was used for transport measurements.  $(\sqrt{7} \times \sqrt{3})$ -In was prepared by depositing approximately three monolayers (MLs) of In on a clean Si(111) surface at 300 K, followed by 600 K annealing for a couple of minutes. The sample quality was confirmed first by the observation of sharp spots in low-energy electron diffraction and then by the sharp electronic states in PES and by the atomic arrangement of an atomically uniform surface with flat terraces in STM. [The obtained STM images were in good agreement with those of  $(\sqrt{7} \times \sqrt{3})$ -In formed by two In layers reported in Refs. [14,23].] PTCDA (purity > 98%) was well degassed in UHV before deposition and deposited on the substrate kept at room temperature with deposition rates slower than 0.3 ML/min. The PTCDA thickness was monitored with a quartz balance and calibrated by PES and

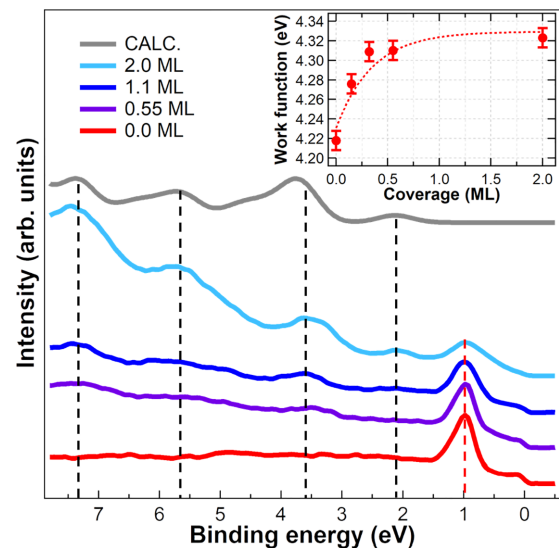


FIG. 1. Coverage-dependent valence band spectra of PTCDA adsorbed  $(\sqrt{7} \times \sqrt{3})$ -In (the four spectra from the bottom) and the calculated DOS of an isolated PTCDA molecule (the uppermost spectrum). The inset shows the change in the work function with respect to the PTCDA coverage.

STM. The sample was maintained below 20 K during all PES measurements and at 4.7 or 80 K in STM. All sample preparation and experiments were performed under UHV conditions.

## III. RESULTS AND DISCUSSION

The PTCDA coverage-dependent valence band spectra obtained with a photon energy  $h\nu$  of 40 eV are shown in Fig. 1. The intensity of the prominent peak observed at a binding energy  $E_B$  of approximately 1 eV (indicated by a red dashed line) on the pristine  $(\sqrt{7} \times \sqrt{3})$ -In decreases, and the intensities of the four peaks at  $E_B \sim 2.1, 3.6, 5.7,$  and  $7.3$  eV (indicated by black dashed lines) develop as the molecular coverage increases. Taking into account the molecular orbital (MO) spectra reported in previous studies [30–32], we attribute the  $E_B \sim 2.1$  eV peak to the highest occupied molecular orbital (HOMO) of PTCDA. Furthermore, by considering the good agreement between the relative  $E_B$  of the observed four peaks and those of the theoretically obtained MOs for an isolated PTCDA molecule (the uppermost spectrum), we conclude that the origin of all four peaks is the MOs of PTCDA. [The calculation was performed using the GAMESS program [33,34] with the Becke three-parameter Lee-Yang-Parr (B3LYP) method and a triple split valence basis set 6-311G\*\*, and the MO energies were shifted so that the HOMO peak coincides with the experimental spectra.] The negligible shift in  $E_B$  of the MOs and the invisible molecule-derived features within the energy gap region of PTCDA, unlike in the case of strongly interacting systems [35], suggest a rather weak interaction between PTCDA and  $(\sqrt{7} \times \sqrt{3})$ -In. This weak interaction is supported by the agreement in work function of the 2 ML PTCDA adsorbed  $(\sqrt{7} \times \sqrt{3})$ -In shown in the inset of Fig. 1 and that of a thick PTCDA film [36]. That is, the very small change in work function at coverages higher than 1 ML indicates that the surface dipole of PTCDA adsorbed

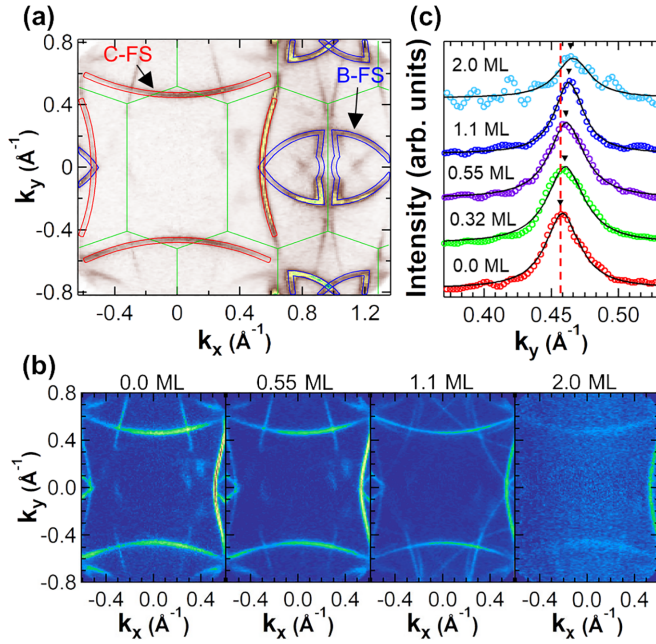


FIG. 2. (a) FS of pristine  $(\sqrt{7} \times \sqrt{3})$ -In. The green solid lines show the  $\sqrt{7} \times \sqrt{3}$  Brillouin zone, and the red and blue solid lines enclose part of the circular and butterfly-shaped FSs, respectively. The  $k_x$  and  $k_y$  axes correspond to the  $[1\bar{1}0]$  and  $[11\bar{2}]$  directions. (b) FSs of PTCDA adsorbed  $(\sqrt{7} \times \sqrt{3})$ -In at different coverages. (c) PTCDA coverage-dependent MDCs obtained from a summation within a  $k_x$  range of  $0 \pm 0.015 \text{ \AA}^{-1}$ . The open circles are the experimental data, and the solid lines overlapping them show the Lorentzian fittings. The peak position in each MDC is indicated by a triangle.

on  $(\sqrt{7} \times \sqrt{3})$ -In and that of a thick PTCDA film are quite similar, and therefore, the charge transfer between PTCDA and  $(\sqrt{7} \times \sqrt{3})$ -In is negligible. Moreover, the negligible shift in  $E_B$  indicates that PTCDA is hardly distorted on  $(\sqrt{7} \times \sqrt{3})$ -In.

The Fermi surfaces (FSs) obtained from a summation of the photoelectron intensity from the Fermi level to  $E_B = 20 \text{ meV}$  with  $h\nu = 40 \text{ eV}$  at different PTCDA coverages are shown in Fig. 2. The FS of the pristine  $(\sqrt{7} \times \sqrt{3})$ -In [Fig. 2(a)], which consists of two types of FSs (a circular FS that is formed mainly by electrons located at the outermost In layer and a butterfly-shaped FS formed mainly by electrons located at the In layer connected to Si), is in good agreement with the experimental and calculated ones reported previously [11,14,18,19,22]. The circular and butterfly-shaped FSs are indicated as C-FS and B-FS, respectively, in Fig. 2. The FSs obtained after PTCDA deposition [Fig. 2(b)] show that the increase in PTCDA coverage leads to an intensity drop of the FS but not to a significant modulation in its shape. (The presence of more FSs at 1.1 ML is due to the existence of two other domains that are rotated  $120^\circ$  each; that is, the sample is a triple-domain  $(\sqrt{7} \times \sqrt{3})$ -In, but this does not affect the discussion.) This result indicates that the interaction between PTCDA and  $(\sqrt{7} \times \sqrt{3})$ -In does not involve chemical bonding and thus hardly affects the electronic structure of  $(\sqrt{7} \times \sqrt{3})$ -In.

TABLE I. Radius of the circular FS at different PTCDA coverages and the estimated number of holes transferred per In atom from the radius.

PTCDA coverage (ML)	Radius ( $\text{\AA}^{-1}$ )	$\Delta$ holes
0.0	$1.4309 \pm 0.0002$	
0.32	$1.4288 \pm 0.0002$	$0.0052 \pm 0.0005$
0.55	$1.4279 \pm 0.0002$	$0.0073 \pm 0.0005$
1.1	$1.4262 \pm 0.0005$	$0.0115 \pm 0.001$
2.0	$1.4233 \pm 0.002$	$0.0184 \pm 0.005$

Figure 2(c) displays the momentum distribution curves (MDCs) at  $k_x = 0$  and  $k_y > 0$ . Hole doping from PTCDA into the In layer would shrink the FSs and thus increase the separation between the two circular FSs at  $k_x = 0$ . As shown in Fig. 2(c), the position of the peak in the MDC, which is obtained by fitting using a Lorentzian function, shows a small shift toward larger  $k_y$  as the PTCDA coverage increases. This means that the adsorbed PTCDA molecules slightly dope holes into the In layer. Table I summarizes the obtained radius of the circular FS at different PTCDA coverages and the number of holes transferred to an In atom from PTCDA estimated from the experimental result. (The number of transferred holes was obtained by comparing the area of the circular FS and the Brillouin zone formed by the In atoms as in Ref. [22].) The amount of hole doping continuously increases even above a PTCDA coverage of 1.0 ML. This results from the fact that PTCDA does not grow layer by layer on  $(\sqrt{7} \times \sqrt{3})$ -In and regions uncovered by PTCDA remain above 1.0 ML, as will be discussed below. Despite its larger electron affinity, the PTCDA adsorption causes less hole doping into  $(\sqrt{7} \times \sqrt{3})$ -In than CuPc. This result indicates that discussing the charge transfer at the interface between organic molecules and metal substrates based on only the energy level alignment is not sufficient.

In order to obtain further information about the interaction between PTCDA and  $(\sqrt{7} \times \sqrt{3})$ -In, we measured the coverage-dependent C 1s and O 1s core levels. In Fig. 3, we show the C 1s and O 1s spectra obtained with  $h\nu = 650 \text{ eV}$  at different PTCDA coverages. Both the C 1s and the O 1s spectra show only an increase in intensity and no remarkable change in the spectral shape as the PTCDA coverage increases.  $E_B$  of the two O 1s components and their relative intensity agree well with those of thick PTCDA films [37–39]. On the other hand, although the relative intensity of the two C 1s components shows agreement with those of thick films [37–39], there is a difference in the  $E_B$  separation. That is, the separation of the two C 1s components in Fig. 3(a) is narrower than those reported in the literature for thick PTCDA films. By considering the origin of the small component at higher  $E_B$ , we conclude that the difference in  $E_B$  separation results from the small charge transfer from In to the carboxylic group, like the case of PTCDA adsorbed on a Sn-covered Si(111) surface [39].

Since the small hole doping and the observation of circular FS even after PTCDA adsorption indicate the possibility of a change in  $T_c$  of  $(\sqrt{7} \times \sqrt{3})$ -In, we performed



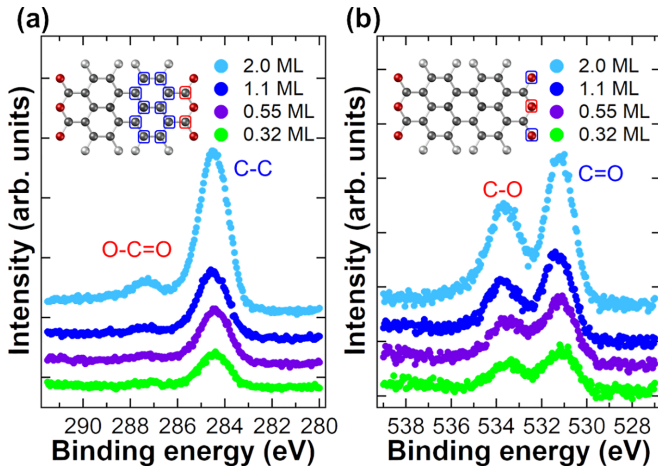


FIG. 3. (a) C 1s and (b) O 1s core-level spectra from PTCDA on  $(\sqrt{7} \times \sqrt{3})$ -In at different coverages. The top left inset in each panel displays the molecular structure of PTCDA with chemically inequivalent C and O atoms.

coverage-dependent transport measurements. The superconducting transition of the pristine  $(\sqrt{7} \times \sqrt{3})$ -In was confirmed by a steep decrease that reaches  $0 \Omega/\square$  in sheet resistance at approximately 3.0 K, which is consistent with previous reports [1–3,20,21]. As shown in Fig. 4(a),  $T_c$  is suppressed when increasing the PTCDA coverage. This is in contrast to the change in  $T_c$  expected from hole doping as in the case of CuPc adsorption [14]. Furthermore, the normal-state sheet resistance at  $\sim 3.5$  K shows a sizable increase after

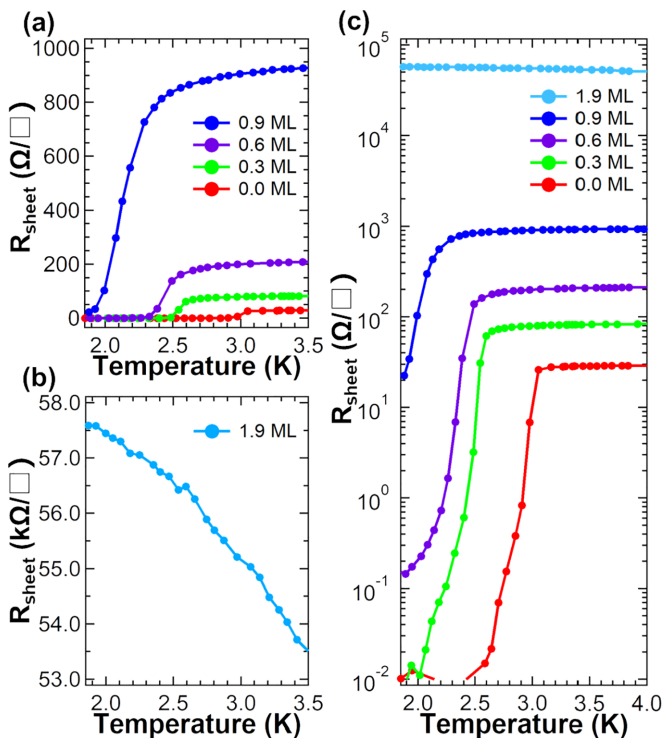


FIG. 4. Temperature-dependent sheet resistance of the PTCDA adsorbed  $(\sqrt{7} \times \sqrt{3})$ -In at PTCDA coverages (a) below 1.0 ML and (b) at 1.9 ML. In (c), the results of (a) and (b) are plotted together with the y axis on a logarithmic scale.

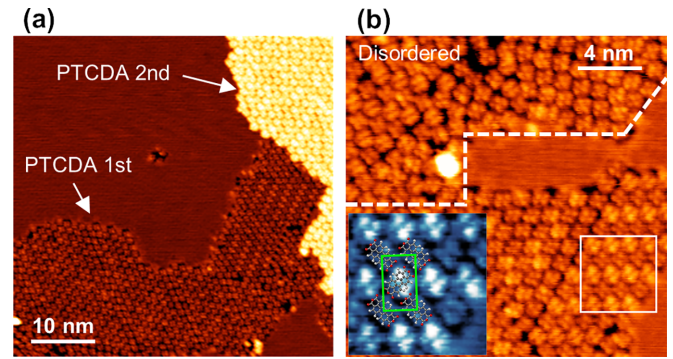


FIG. 5. STM image of the 1.0 ML PTCDA adsorbed  $(\sqrt{7} \times \sqrt{3})$ -In. The sample bias and tunnel current are  $-2.0$  V and 10 pA. (a) A  $50 \times 50 \text{ nm}^2$  STM image. The two white arrows indicate the regions covered with one and two PTCDA layers. (b) Closer view of the first PTCDA layer. Regions of ordered and disordered PTCDA molecules are shown below and above the white dashed line. The inset shows an enlarged view of the  $5 \times 5 \text{ nm}^2$  area outlined by the white solid square, where PTCDA molecules form an ordered herringbone structure. The green rectangle in the inset indicates the unit cell.

PTCDA adsorption, which was not observed in the case of metal-phthalocyanine adsorptions [14,23–25], and the disappearance of superconductivity and an increase in sheet resistance when decreasing temperature at 1.9 ML [Fig. 4(b)] reveal the semiconducting or insulating behavior of  $(\sqrt{7} \times \sqrt{3})$ -In at this coverage.

The evolution of temperature dependence of sheet resistance is displayed in Fig. 4(c). Since the ARPES measurements confirm that the electronic structure is modified by only a small amount of hole doping and the metallic bands still remain up to 2.0 ML, this transition in conductivity would not be a phase transition accompanied with a gap opening at the Fermi level. It should be noted that the sheet resistance increases up to more than  $50 \text{ k}\Omega/\square$ , which drastically exceeds the universal critical sheet resistance  $h/4e^2$  ( $= 6.45 \text{ k}\Omega/\square$ ) of the superconductor-insulator transition in the 2D limit [40–42]. Since PTCDA has no spin states, the magnetic effects cannot be the origin of the suppression in superconductivity. In superconducting thin films,  $T_c$  has been reported to decrease, and the sheet resistance has been reported to increase in the presence of disorder [40,42]. This means that one possible origin of the results shown in Fig. 4 would be a disordered potential formed on  $(\sqrt{7} \times \sqrt{3})$ -In by the adsorbed PTCDA.

Figure 5(a) shows a  $50 \times 50 \text{ nm}^2$  STM image of  $(\sqrt{7} \times \sqrt{3})$ -In covered with 1.0 ML of PTCDA. The coexistence of the first and second PTCDA layers and the presence of uncovered  $(\sqrt{7} \times \sqrt{3})$ -In regions indicates that the PTCDA deposition follows an island growth mode and not a layer-by-layer one as in the case of CuPc. This suggestion is consistent with the PES results discussed above, in which the amount of hole doping does not saturate and/or show a maximum at a PTCDA coverage of 1 ML. [The PTCDA molecules of the first layers appear as dark as the  $(\sqrt{7} \times \sqrt{3})$ -In region in the STM image, but since no significant changes are observed in the electronic structure of  $(\sqrt{7} \times \sqrt{3})$ -In upon PTCDA adsorption, this is due to an effect of the electronic states of PTCDA and does not indicate the molecule is at the same

height as the In layer.] The STM image with molecular resolution of the first PTCDA layer reveals a mixture of ordered and disordered regions [Fig. 5(b)]. This means that PTCDA molecules do not form a perfectly ordered molecular layer on  $(\sqrt{7} \times \sqrt{3})$ -In like metal-phthalocyanine molecules [14,23–25]. In both regions, PTCDA molecules are flat lying like PTCDA adsorbed on various substrates [27].

As shown in the inset of Fig. 5(b), PTCDA molecules form a herringbone structure in the ordered region, which is commonly seen in the first few layers on metal substrates [32,43,44] or metal-terminated semiconductor surfaces [45–47]. On the other hand, PTCDA molecules are randomly arranged in the disordered region. The disruption in ordering might be due to the defects of the substrate surface that act as trapping sites and cause different interactions with the surrounding molecules. In the herringbone structure, the electropositive H atoms of PTCDA always face the electronegative O atoms of the neighboring molecule and cancel out the charge distribution within the molecule. In the disordered region, however, the charge distribution cannot be canceled and thus would induce a random electrostatic potential in the underlying In layer. This would lead the PTCDA molecules to play a role as electron scatterers that cause carrier localization in the 2D In layer [48,49]. We therefore conclude that the observed suppression in superconductivity, increase in normal-state sheet resistance, and insulating transition in conductivity result from the random potential induced by disordered PTCDA molecules. This result provides new insight into a rational design for enhancing the superconducting properties of ALSCs.

#### IV. CONCLUSIONS

In conclusion, we have measured the coverage-dependent electronic structure, resistivity, and molecular arrangement of

PTCDA adsorbed  $(\sqrt{7} \times \sqrt{3})$ -In to understand the effect of organic molecular adsorption on an ALSC. The FSs at different PTCDA coverages indicate that the adsorption causes a slight hole doping into  $(\sqrt{7} \times \sqrt{3})$ -In without making an appreciable alteration to its electronic structure. Regarding the transport measurements, a suppression of  $T_c$  with an increase in the normal-state sheet resistance, followed by an insulating transition, was observed when increasing the PTCDA coverage, although the hole doping and the absence of spin states in the molecule were expected to increase  $T_c$ . The unexpected results in conductivity come from the presence of disordered PTCDA molecules on  $(\sqrt{7} \times \sqrt{3})$ -In, which induces random potentials and thus leads to the localization of conduction electrons in the In layer. This shows that the 2D superconductivity is destroyed due to potential disordering introduced by molecular adsorption and therefore indicates the importance of the high crystallinity of a 2D molecular film in 2D systems consisting of an ALSC and organic molecules.

#### ACKNOWLEDGMENTS

This work was supported by JSPS KAKENHI Grants No. JP22H01957, No. JP22H01961, No. JP20H02707, No. JP19H02592, and No. JP20H05621, the World Premier International Research Center (WPI) Initiative on Materials Nano-architectonics, and the Spintronics Research Network of Japan (Spin-RNJ). We acknowledge MAX IV Laboratory for time on Beamline Bloch under Proposal No. 20200385. Research conducted at MAX IV, a Swedish national user facility, is supported by the Swedish Research council under Contract No. 2018-07152, the Swedish Governmental Agency for Innovation Systems under Contract No. 2018-04969, and Formas under Contract No. 2019-02496.

- 
- [1] T. Zhang, P. Cheng, W. J. Li, Y. J. Sun, G. Wang, X. G. Zhu, K. He, L. Wang, X. Ma, X. Chen, Y. Wang, Y. Liu, H. Q. Lin, J. F. Jia, and Q. K. Xue, Superconductivity in one-atomic-layer metal films grown on Si(111), *Nat. Phys.* **6**, 104 (2010).
  - [2] T. Uchihashi, P. Mishra, M. Aono, and T. Nakayama, Macroscopic Superconducting Current through a Silicon Surface Reconstruction with Indium Adatoms: Si(111)- $(\sqrt{7} \times \sqrt{3})$ -In, *Phys. Rev. Lett.* **107**, 207001 (2011).
  - [3] M. Yamada, T. Hirahara, and S. Hasegawa, Magnetoresistance Measurements of a Superconducting Surface State of In-Induced and Pb-Induced Structures on Si(111), *Phys. Rev. Lett.* **110**, 237001 (2013).
  - [4] A. V. Matetskiy, S. Ichinokura, L. V. Bondarenko, A. Y. Tupchaya, D. V. Gruznev, A. V. Zotov, A. A. Saranin, R. Hobara, A. Takayama, and S. Hasegawa, Two-Dimensional Superconductor with a Giant Rashba Effect: One-Atom-Layer Tl-Pb Compound on Si(111), *Phys. Rev. Lett.* **115**, 147003 (2015).
  - [5] C. Brun, T. Cren, and D. Roditchev, Review of 2D superconductivity: The ultimate case of epitaxial monolayers, *Supercond. Sci. Technol.* **30**, 013003 (2017).
  - [6] T. Uchihashi, Two-dimensional superconductors with atomic-scale thickness, *Supercond. Sci. Technol.* **30**, 013002 (2017).
  - [7] J. Bardeen, L. N. Cooper, and J. R. Schrieffer, Theory of superconductivity, *Phys. Rev.* **108**, 1175 (1957).
  - [8] T. Sekihara, R. Masutomi, and T. Okamoto, Two-Dimensional Superconducting State of Monolayer Pb Films Grown on GaAs(110) in a Strong Parallel Magnetic Field, *Phys. Rev. Lett.* **111**, 057005 (2013).
  - [9] C. Brun, T. Cren, V. Cherkez, F. Debontridder, S. Pons, D. Fokin, M. C. Tringides, S. Bozhko, L. B. Ioffe, B. L. Altshuler, and D. Roditchev, Remarkable effects of disorder on superconductivity of single atomic layers of lead on silicon, *Nat. Phys.* **10**, 444 (2014).
  - [10] T. Nakamura, H. Kim, S. Ichinokura, A. Takayama, A. V. Zotov, A. A. Saranin, Y. Hasegawa, and S. Hasegawa, Unconventional superconductivity in the single-atom-layer alloy Si(111)- $\sqrt{3} \times \sqrt{3}$ -(Tl, Pb), *Phys. Rev. B* **98**, 134505 (2018).
  - [11] S. Yoshizawa, T. Kobayashi, Y. Nakata, K. Yaji, K. Yokota, F. Komori, S. Shin, K. Sakamoto, and T. Uchihashi, Atomic-layer Rashba-type superconductor protected by dynamic spin momentum locking, *Nat. Commun.* **12**, 1462 (2021).

- [12] M. Smidman, M. B. Salamon, H. Q. Yuan, and D. F. Agterberg, Superconductivity and spin-orbit coupling in non-centrosymmetric materials: A review, *Rep. Prog. Phys.* **80**, 036501 (2017).
- [13] G. C. Ménard, S. Guissart, C. Brun, R. T. Leriche, M. Trif, F. Debontridder, D. Demaille, D. Roditchev, P. Simon, and T. Cren, Two-dimensional topological superconductivity in Pb/Co/Si(111), *Nat. Commun.* **8**, 2040 (2017).
- [14] S. Yoshizawa, E. Minamitani, S. Vijayaraghavan, P. Mishra, Y. Takagi, T. Yokoyama, H. Oba, J. Nitta, K. Sakamoto, S. Watanabe, T. Uchihashi, Controlled modification of superconductivity in epitaxial atomic layer-organic molecule heterostructures, *Nano Lett.* **17**, 2287 (2017).
- [15] J. W. Park and M. H. Kang, Double-Layer In Structural Model for the In/Si(111)- $\sqrt{7} \times \sqrt{3}$  Surface, *Phys. Rev. Lett.* **109**, 166102 (2012).
- [16] K. Uchida and A. Oshiyama, Identification of metallic phases of In atomic layers on Si(111) surfaces, *Phys. Rev. B* **87**, 165433 (2013).
- [17] T. Shirasawa, S. Yoshizawa, T. Takahashi, and T. Uchihashi, Structure determination of the Si(111)- $\sqrt{7} \times \sqrt{3}$ -In atomic-layer superconductor, *Phys. Rev. B* **99**, 100502(R) (2019).
- [18] E. Rotenberg, H. Koh, K. Rossnagel, H. W. Yeom, J. Schäfer, B. Krenzer, M. P. Rocha, and S. D. Kevan, Indium  $\sqrt{7} \times \sqrt{3}$  on Si(111): A Nearly Free Electron Metal in Two Dimensions, *Phys. Rev. Lett.* **91**, 246404 (2003).
- [19] T. Kobayashi, Y. Nakata, K. Yaji, T. Shishidou, D. Agterberg, S. Yoshizawa, F. Komori, S. Shin, M. Weinert, T. Uchihashi, and K. Sakamoto, Orbital Angular Momentum Induced Spin Polarization of 2D Metallic Bands, *Phys. Rev. Lett.* **125**, 176401 (2020).
- [20] T. Uchihashi, P. Mishra, and T. Nakayama, Resistive phase transition of the superconducting Si(111)-( $\sqrt{7} \times \sqrt{3}$ )-In surface, *Nanoscale Res. Lett.* **8**, 167 (2013).
- [21] S. Yoshizawa, H. Kim, T. Kawakami, Y. Nagai, T. Nakayama, X. Hu, Y. Hasegawa, and T. Uchihashi, Imaging Josephson Vortices on the Surface Superconductor Si(111)-( $\sqrt{7} \times \sqrt{3}$ )-In using a Scanning Tunneling Microscope, *Phys. Rev. Lett.* **113**, 247004 (2014).
- [22] R. Sagehashi, T. Kobayashi, T. Uchihashi, and K. Sakamoto, Tuning the Fermi surface of In/Si(111)-( $\sqrt{7} \times \sqrt{3}$ ) by CuPc adsorption, *Surf. Sci.* **705**, 121777 (2021).
- [23] N. Sumi, Y. Yamada, M. Sasaki, R. Arafune, N. Takagi, S. Yoshizawa, and T. Uchihashi, Unsubstituted and fluorinated copper phthalocyanine overlayers on Si(111)-( $\sqrt{7} \times \sqrt{3}$ )-In surface: Adsorption geometry, charge polarization, and effects on superconductivity, *J. Phys. Chem. C* **123**, 8951 (2019).
- [24] T. Uchihashi, S. Yoshizawa, E. Minamitani, S. Watanabe, Y. Takagi, and T. Yokoyama, Persistent superconductivity in atomic layer-magnetic molecule van der Waals heterostructures: A comparative study, *Mol. Syst. Des. Eng.* **4**, 511 (2019).
- [25] K. Yokota, S. Inagaki, W. Qian, R. Nemoto, S. Yoshizawa, E. Minamitani, K. Sakamoto, and T. Uchihashi, Non-charge-transfer origin of Tc enhancement in a surface superconductor Si(111)-( $\sqrt{7} \times \sqrt{3}$ )-In with adsorbed organic molecules, *J. Phys. Soc. Jpn.* **91**, 123704 (2022).
- [26] E. Umbach, C. Seidel, J. Taborski, R. Li, and A. Soukopp, Highly-ordered organic adsorbates: Commensurate superstructures, OMBE, and 1D nanostructures, *Phys. Status Solidi B* **192**, 389 (1995).
- [27] N. Nicoara, J. M. Gómez-Rodríguez, and J. Méndez, Growth of PTCDA films on various substrates studied by scanning tunneling microscopy and spectroscopy, *Phys. Status Solidi B* **256**, 1800333 (2019).
- [28] P. C. Rusu, G. Giovannetti, C. Weijtens, R. Coehoorn, and G. Brocks, First-principles study of the dipole layer formation at metal-organic interfaces, *Phys. Rev. B* **81**, 125403 (2010).
- [29] W. Wu, L. A. Rochford, S. Felton, Z. Wu, J. L. Yang, S. Heutz, G. Aeppli, T. S. Jones, N. M. Harrison, and A. J. Fisher, Magnetic properties of copper hexadecaphthalocyanine (F<sub>16</sub>CuPc) thin films and powders, *J. Appl. Phys.* **113**, 013914 (2013).
- [30] D. R. T. Zahn, G. N. Gavrila, and M. Gorgoi, The transport gap of organic semiconductors studied using the combination of direct and inverse photoemission, *Chem. Phys.* **325**, 99 (2006).
- [31] J. B. Gustafsson, E. Moons, S. M. Widstrand, M. Gurnett, and L. S. O. Johansson, Thin PTCDA films on Si(001): 2. Electronic structure, *Surf. Sci.* **572**, 32 (2004).
- [32] Y. Zou, L. Kilian, A. Schöll, T. Schmidt, R. Fink, and E. Umbach, Chemical bonding of PTCDA on Ag surfaces and the formation of interface states, *Surf. Sci.* **600**, 1240 (2006).
- [33] M. W. Schmidt, K. K. Baldrige, J. A. Boatz, S. T. Elbert, M. S. Gordon, J. H. Jensen, S. Koseki, N. Matsunaga, K. A. Nguyen, S. Su, T. L. Windus, M. Dupuis, and J. A. Montgomery, General atomic and molecular electronic structure system, *J. Comput. Chem.* **14**, 1347 (1993).
- [34] G. M. J. Barca *et al.*, Recent developments in the general atomic and molecular electronic structure system, *J. Chem. Phys.* **152**, 154102 (2020).
- [35] S. Duhm, A. Gerlach, I. Salzmann, B. Bröker, R. Johnson, F. Schreiber, and N. Koch, PTCDA on Au(111), Ag(111) and Cu(111): Correlation of interface charge transfer to bonding distance, *Org. Electron.* **9**, 111 (2008).
- [36] M. S. Khoshkhoo, H. Peisert, T. Chassé, and M. Scheele, The role of the density of interface states in interfacial energy level alignment of PTCDA, *Org. Electron.* **49**, 249 (2017).
- [37] A. Schöll, Y. Zou, M. Jung, T. Schmidt, R. Fink, and E. Umbach, Line shapes and satellites in high-resolution x-ray photoelectron spectra of large  $\pi$ -conjugated organic molecules, *J. Chem. Phys.* **121**, 10260 (2004).
- [38] J. B. Gustafsson, H. M. Zhang, E. Moons, and L. S. O. Johansson, Electron spectroscopy studies of PTCDA on Ag/Si(111)- $\sqrt{3} \times \sqrt{3}$ , *Phys. Rev. B* **75**, 155413 (2007).
- [39] H. M. Zhang and L. S. O. Johansson, Electronic structure of PTCDA on Sn/Si(111)- $2\sqrt{3} \times 2\sqrt{3}$ , *Chem. Phys.* **439**, 71 (2014).
- [40] D. B. Haviland, Y. Liu, and A. M. Goldman, Onset of Superconductivity in the Two-Dimensional Limit, *Phys. Rev. Lett.* **62**, 2180 (1989).
- [41] T. Pang, Universal Critical Normal Sheet Resistance in Ultrathin Films, *Phys. Rev. Lett.* **62**, 2176 (1989).
- [42] A. M. Goldman and N. Marković, Superconductor-insulator transitions in the two-dimensional limit, *Phys. Today* **51**(11), 39 (1998).
- [43] T. Schmitz-Hübsch, T. Fritz, F. Sellam, R. Staub, and K. Leo, Epitaxial growth of 3,4,9,10-perylene-tetracarboxylic-dianhydride on Au(111): A STM and RHEED study, *Phys. Rev. B* **55**, 7972 (1997).
- [44] T. Wagner, A. Bannani, C. Bobisch, H. Karacuban, and R. Möller, The initial growth of PTCDA on Cu(111) studied by STM, *J. Phys.: Condens. Matter* **19**, 056009 (2007).

- [45] J. B. Gustafsson, H. M. Zhang, and L. S. O. Johansson, STM studies of thin PTCDA films on Ag/Si(111)- $\sqrt{3} \times \sqrt{3}$ , *Phys. Rev. B* **75**, 155414 (2007).
- [46] D. Shin, Z. Wei, H. Shim, and G. Lee, Adsorption and ordering of PTCDA on various reconstruction surfaces of In/Si(111), *Appl. Surf. Sci.* **372**, 87 (2016).
- [47] N. Nicoara, J. Méndez, and J. M. Gómez-Rodríguez, Growth of ordered molecular layers of PTCDA on Pb/Si(111) surfaces: A scanning tunneling microscopy study, *Nanotechnology* **27**, 365706 (2016).
- [48] P. W. Anderson, Absence of diffusion in certain random lattices, *Phys. Rev.* **109**, 1492 (1958).
- [49] E. Abrahams, P. W. Anderson, D. C. Licciardello, and T. V. Ramakrishnan, Scaling Theory of Localization: Absence of Quantum Diffusion in Two Dimensions, *Phys. Rev. Lett.* **42**, 673 (1979).